Dyes and Pigments 87 (2010) 144–148

Contents lists available at ScienceDirect

Dyes and Pigments

journal homepage: www.elsevier.com/locate/dyepig

The electrical conductivity and dielectric properties of C.I. Basic Violet 10

Sh.A. Mansour [a,*], I.S. Yahia [b], F. Yakuphanoglu [c]

[a] Basic Engineering Science Department, Faculty of Engineering, Menofia University, Shebin El-Kom, Egypt
[b] Department of Physics, Faculty of Education, Ain Shams University, Roxy, Cairo, Egypt
[c] Department of Physics, Faculty of Arts and Sciences, Firat University, Elazig, Turkey

ARTICLE INFO

Article history:
Received 22 August 2009
Received in revised form
10 March 2010
Accepted 13 March 2010
Available online 21 March 2010

Keywords:
Organic semiconductor
Organic dye
Dielectric relaxation

ABSTRACT

The electrical and dielectrical properties of C.I. Basic Violet 10 were investigated using both DC and AC measurements. The DC electrical conductivity of the dye exhibited similar behavior to that of organic semiconductors and the mechanism of the AC conductivity the dye can be attributed to correlated barrier hopping, as confirmed by an observed reduction in activation energy. The density of localized states for C.I. Basic Violet 10 was 0.15×10^{22} to 4.4×10^{22} eV^{-1} cm^{-3} over the range of temperatures and frequencies employed. Variation of the dielectric constant with temperature at different frequencies showed a dielectric relaxation peak; with increasing frequency, the intensity of the dielectric relaxation peak decreased and became less pronounced. The obtained results suggest that C.I. Basic Violet 10 is an organic semiconductor and its dielectric relaxation mechanism is temperature-dependent.

1. Introduction

Rhodamine dyes enjoy manifold biotechnological applications such as fluorescence microscopy, flow cytometry, fluorescence correlation spectroscopy and enzyme-linked immunosorbent assay (ELISA) [1–3]. Such dyes, as exemplified by C.I. Basic Violet 10, are excellent candidates for the construction of an OFF/On- type fluorescent probe due to its excellent spectroscopic properties of large molar extinction coefficient, visible wavelength excitation and high fluorescence quantum yield [4]. Several rhodamine based fluorescent chemo-sensors have recently been reported for determining Fe^{3+}, Cu^{2+}, Cr^{3+} and Hg^{2+} ions in living cells [5] and a Sn/rhodamine-101/p-Si Schottky diode was fabricated using Rhodamine-101 [6].

Recent interest in thin organic semiconducting films has arisen because of their application in optical and electronic devices; indeed, all types of electronic devices, such as organic thin film transistors, printable circuits, organic capacitors, and organic photovoltaic devices have received much attention in the past few years [6].

To determine the electrical conductivity and dielectric mechanism of organic semiconductors, low frequency conductivity and dielectric measurements provide additional information on the conductivity mechanism as well as direct current conductivity, as the both direct and alternating current (DC and AC) electrical properties of organic and inorganic materials provide important information about the conduction process and the predominant charge transport mechanism within an organic material. These measurements are the major tools used for the study of ionic conduction in glasses, ceramics and organic materials [7–9].

The paper concerns the DC and AC current conductivity and dielectric properties of C.I. Basic Violet 10 and an investigation as to whether the dye constitutes an organic semiconductor applicable to organic devices. Measurements were made using pellets of the dye as the conductivity data of organic semiconductors is frequently obtained by measuring the DC conductivity of compressed powder samples [10–13]. It is observed that the conductivity–temperature profile of both film and pellet samples are similar, regardless of the form of the sample [14]. This procedure assumes the elimination of interparticle contact resistance due to pressure application [15].

2. Experimental

C.I. Basic Violet 10, [9-(2-carboxyphenyl)-6-diethylamino-3-xanthenylidene]-diethylammonium chloride] (Fig. 1) was obtained from Aldrich in with high purity. For electrical conductivity measurements, pellets (3.55 mm of radius 0.66 cm) of the dye were formed via the application of 500 kg/cm^2. The dye pellet was sandwiched between two Cu electrodes using a specially designed holder.

A programmable, automatic RLC bridge (PM 6304 Philips) was used to measure the impedance Z, capacitance *C* and loss tangent

* Corresponding author. Tel.: +20 20226843645; fax: +20 0482235695.
E-mail address: shehab_mansour@yahoo.com (Sh.A. Mansour).

0143-7208/$ – see front matter © 2010 Elsevier Ltd. All rights reserved.
doi:10.1016/j.dyepig.2010.03.011

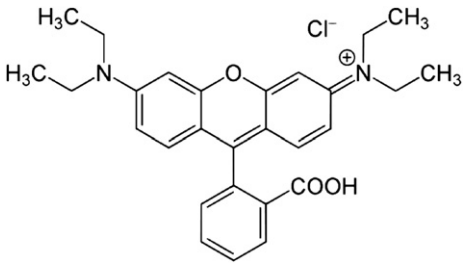

Fig. 1. The chemical structure of C.I. Basic Violet 10.

(tan δ) directly. The DC electrical resistance R for the investigated sample was measured using a KEITHLEYE 616 a digital electrometer in a shielded furnace. Temperature was measured using a calibrated Chromel–Alumel thermocouple connected to a digital multimeter (HC-5010-EC).

3. Results and discussion

3.1. DC and AC electrical conductivities of C.I. Basic Violet 10

The electrical conductivity dependence on temperature is shown in Fig. 2 from which it is apparent that there were two linear regions, suggesting the presence of two different conduction mechanisms operating at low temperature, in the range 303–373 K and at high temperature in the range 373–423 K owing to the presence of different energy levels in the dye. The DC conductivity mechanism of the sample can be analyzed using the well-known Arrhenius equation:

$$\sigma_{dc} = \sigma_o \exp(-\Delta E_\sigma / k_B T), \quad (1)$$

where ΔE_σ is the activation energy for electrical conduction, T is the absolute temperature, k_B is the Boltzmann's constant and σ_o is the pre-exponential factor, including the charge carrier mobility and density of states. The activation energy values for the conductivity regions ($\Delta E_{\sigma 1}$ for region I and $\Delta E_{\sigma 2}$ for region II) were found to be 0.16 eV and 0.42 eV, respectively. Room temperature conductivity of the investigated sample was found to be 2.35×10^{-11} (Ω^{-1} cm^{-1}). The electrical conductivity of the dye increased with increasing temperature, indicating that the electrical conductivity mechanism is similar to that of semiconductors and the obtained electronic parameters confirm that the dye is an organic semiconductor in terms of its electronic parameters [16]. The increase in conductivity with increase in temperature implies that as temperature is increased, more charge carriers overcome the activation energy barrier and participate in electrical conduction. It is believed that two types of conduction mechanism occur, namely one in the first conduction region (I) and the other in the second conduction region (II). In both regions I and II, electrical conductivity is thermally activated owing to thermal excitation of charge carriers by changing the activation energy [17]. The observed increase in conduction can be associated with the number of π-electrons of the compound, when activation energy may also be related to electron activation within the structure. The π-electron mobility and the semiconduction behaviour of C.I. Basic Violet 10 dye result from the transfer of π-electrons [18].

The AC conductivity dependence of frequency can be expressed by the following relation [19–22]:

$$\sigma_{ac}(\omega) = A\omega^s \quad (2)$$

where, A is a constant, ω is the angular frequency and s a parameter which determines AC conduction. Fig. 3 shows the frequency

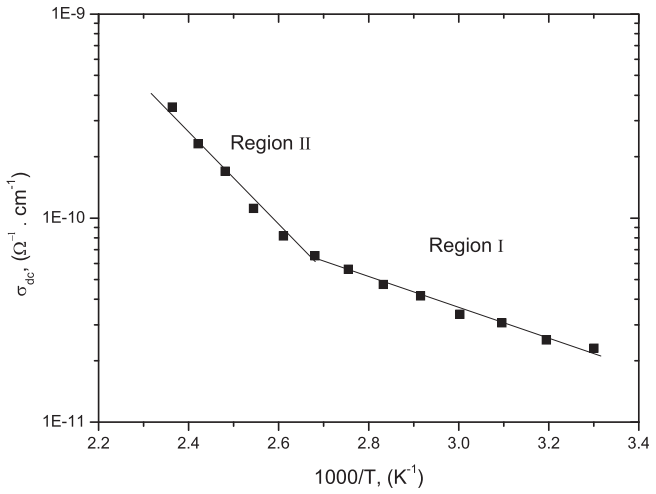

Fig. 2. Temperature dependence of the dc electrical conductivity of the C.I. Basic Violet 10 dye. The solid lines represented least-squares fitting.

dependence of the AC conductivity at different temperatures from which it is clear that σ_{ac} (ω) increased linearly with increasing frequency. The frequency exponent values s were calculated from the slopes of Fig. 2 [16–19]. The change of s with temperature is shown in Fig. 4 from which it is apparent that the values of s decreased with increasing temperature.

According to the quantum mechanical tunneling (QMT) model [23], the exponent s is ~0.8 and increases slightly in both the absence and presence of increasing temperature; hence, the QMT model was not considered applicable to the results obtained. In the non-overlapping small Polarons (NSPT) model, the exponent s is dependent upon temperature insofar as it increases with increasing temperature; thus, the NSPT model was not applicable to the obtained results [24]. According to the overlapping-large polaron tunneling (OLPT) model [25], the exponent s is both temperature and frequency dependent and s decreases with increasing temperature, reaching a minimum value at a given temperature before continuing to increase with increasing temperature. Hence, the OLPT model was deemed to be unapplicable to the results obtained. However, in the correlated barrier hopping (CBH) model, s decreases with increasing temperature, which is in good agreement with the obtained results, as shown in Fig. 4. Thus, the

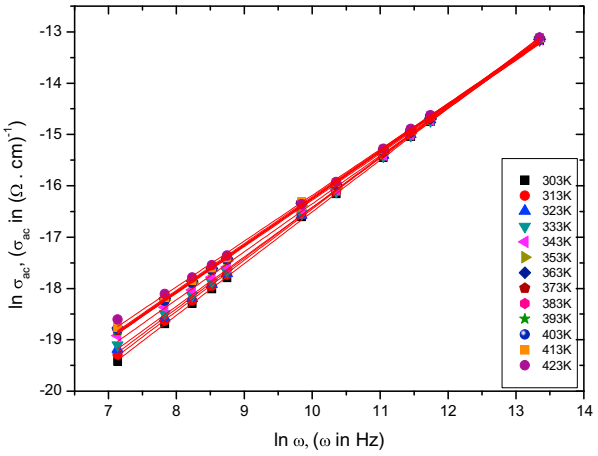

Fig. 3. Frequency dependence of σ_{ac} (ω) for the C.I. Basic Violet 10 dye at different temperatures. The solid lines represented least-squares fitting.

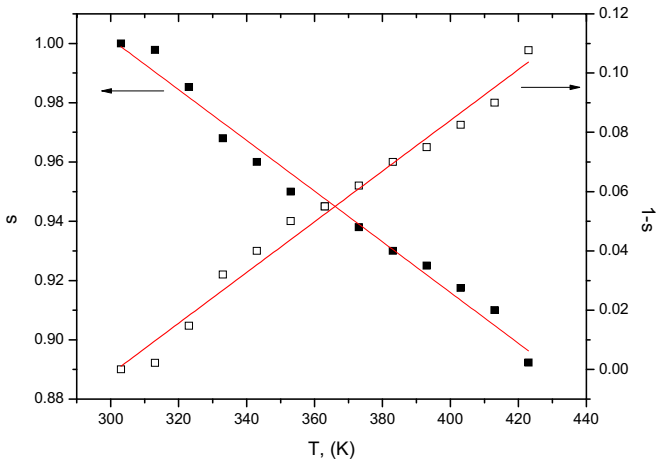

Fig. 4. Temperature dependence of the frequency exponent s and the $1 - s$ for the C.I. Basic Violet 10 dye. The solid lines represented least-squares fitting.

frequency dependence of σ_{ac} (ω) observed for the dye can be explained in terms of the CBH model as developed by Pike [26] for single-electron hopping and extended by Elliot [27,28]. In this model, carrier motion occurs by means of hopping over the coulomb barrier that separates two defect centers. Coulombic correlation between the charged defect centers results in the relaxation variable W of the coulomb barrier and the intersite separation R. In this model, the height of the barrier can be defined as

$$W = W_m - ne^2/\pi\varepsilon_1(\omega)\varepsilon_0 R, \tag{3}$$

where W is the height of barrier, e is the electronic charge, ε_1 (ω) the dielectric constant of the material, ε_0 the dielectric permittivity of free space and n the number of electrons able to hop (the density of pair sites) ($n = 1$ for a single polaron and $n = 2$ for a bipolaron). In the CBH model, s is expressed by the following relation,

$$s = 1 - 6k_B T/[W_m - k_B T \ln(\omega\tau_0)] \tag{4}$$

where τ_o is the characteristic relaxation time, which is in the order of atomic vibrational period $\tau_o = 10^{-13}$ s. It is worth mentioning that, at least for small values of W_m/k_BT, s increases with increasing frequency but for large values of W_m/k_BT, s approaches unity but the increase is so small that s is effectively independent of frequency. hence, Eq. (4) can be reduced to [29],

$$1 - s = 6k_B T/W_m \tag{5}$$

To calculate the W_m (the binding energy of the carrier in its localized sites), the curve of $1 - s$ vs. T was plotted. The obtained data for the sample are shown in Fig. 4 and its slope is used to calculate the binding energy W_m i.e., the binding energy W_m is related to the maximum barrier height at infinite interstatic separation, which is called the polaron binding energy, i.e. the binding energy of the carrier in its localized site.

According to the Austin–Mott formula [30] based on CBH model, ac conductivity σ_{ac} (ω) can be explained in terms of hopping of electrons between a pair of localized states N (E_F) at the Fermi level E_F. σ_{ac} (ω) is related to the number of sites per unit energy per unit volume N (E_F) at the Fermi level as given by:

$$\sigma_{ac}(\omega) = \left(\frac{\pi}{3}\right)[N(E_F)]^2 T k_B e^2 \alpha^{-5} \omega [\ln(\nu_{ph}/\omega)]^4 \tag{6}$$

where α is the exponential decay parameter of localized states wave functions ($\alpha^{-1} = 10$ Å), ν_{ph} is the characteristic phonon frequency ($\nu_{ph} = 10^{12}$ s^{-1}), N (E_F) is the density of states near the Fermi level, $\omega = 2\pi f$ and f is the measured frequency. The density of localized states N (E_F) for different temperatures and frequencies was evaluated using Eq. (6). The values of N (E_F) are of order of $0.15 \times 10^{22} - 4.4 \times 10^{22}$ eV^{-1} cm^{-3} in the studied range of temperatures. The values of N (E_F) increase with temperature, confirming that the electrical conductivity increases with temperature.

Temperature dependence of the ac conductivity σ_{ac} (ω) at different frequencies was shown in Fig. 5. It is seen that σ_{ac} (ω) increases linearly with the reciprocal of absolute temperature. This dependence of ac conductivity on temperature suggests that the ac conductivity is controlled by thermally activated process and it can be analyzed according to the well-known Arrhenius equation:

$$\sigma_{ac}(\omega) = \sigma_o \exp(-\Delta E(\omega)/k_B T) \tag{7}$$

where σ_o is constant, ΔE (ω) is the activation energy for electrical conduction. The ac activation energy of conduction is calculated for different frequencies from the slopes of the straight lines of Fig. 5. The frequency dependence of the ac activation energy ΔE (ω) for the dye is shown in Fig. 6. It is clear from this figure that ΔE (ω) decreases with increasing frequency. Such a decrease can be attributed to the contribution of the frequency applied to the conduction mechanism, which confirms the hopping conduction to be the dominant mechanism. The ΔE (ω) values for the samples decrease with increasing frequency. The increase of the applied field frequency enhances the electronic jumps between the localized states and in turn, the activation energy ΔE (ω) decreases with increasing frequency [31,32].

3.2. Dielectric properties of C.I. Basic Violet 10

Studies of the frequency dependent electrical conductivity of semiconductor materials are important to explain the mechanisms of conduction in these materials. The dielectric relaxation studies are important to understand the nature and the origin of dielectric losses, which in turn, may be useful in the determination of the structure and defects in solids. The complex dielectric function for the investigated organic dye is expressed as [33,34]:

$$\varepsilon^*(\omega) = \varepsilon_1(\omega) + i\varepsilon_2(\omega), \tag{8}$$

where ε_1 (ω) and ε_2 (ω) are the real and imaginary part of the dielectric constant, respectively. The real and imaginary parts of the

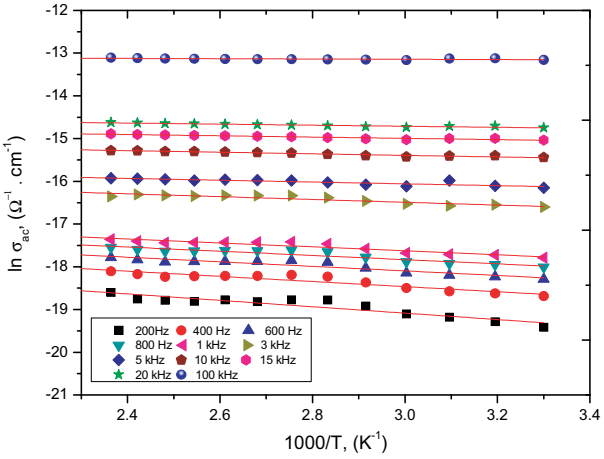

Fig. 5. The temperature dependence of ac conductivity for C.I. Basic Violet 10 dye. The solid lines represented least-squares fitting.

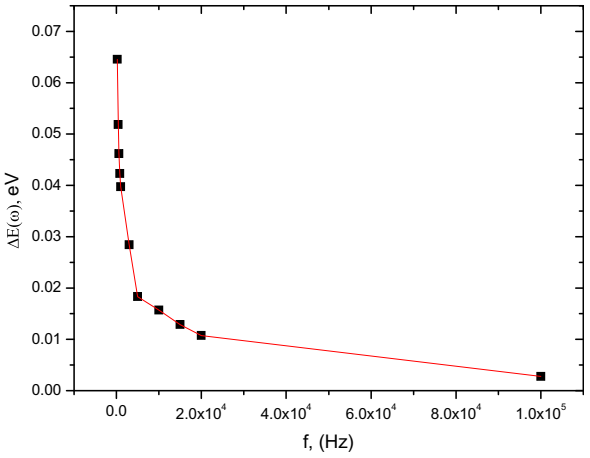

Fig. 6. The frequency dependence of ac activation energy for C.I. Basic Violet 10 dye.

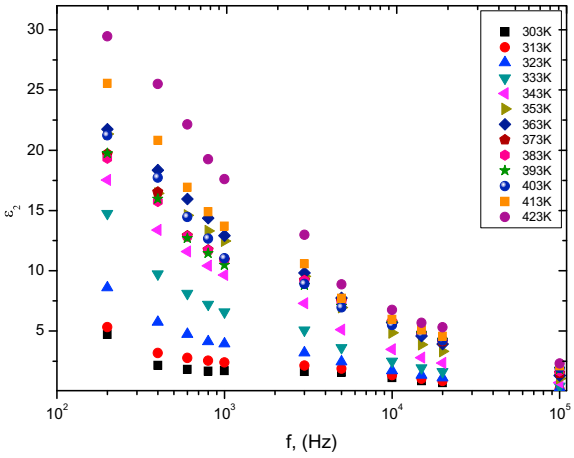

Fig. 8. The frequency dependence of ε_2 (ω) at different temperatures for C.I. Basic Violet 10 dye.

dielectric constant were determined from the measurements of the capacitance C and loss tangent tan δ under different temperatures and frequencies. Figs. 7 and 8 shows the variation of ε_1 (ω) and ε_2 (ω) with frequency at different temperatures, respectively. As seen in Figs. 7 and 8, ε_1 (ω) and ε_2 (ω) decrease with increasing frequency. This can be explained by means of the dielectric polarization mechanism of the material. Dielectric polarization occurs as electronic, ionic, interfacial or dipolar polarization. Electronic and ionic polarizations are active in the high frequency range, while the other two mechanisms prevail in the low frequency range. The increase of both ε_1 (ω) and ε_2 (ω) towards the low frequency region may be attributed to interfacial polarization which occurs via space charges formed in the material induce image charges on electrodes. In the presence of an effective electric field, these space charges which migrate are trapped by defects and a localized accumulation of charge is formed at the electrode and sample interface, consequently ε_1 (ω) and ε_2 (ω) shows higher value at low frequencies [35–37].

The increase of ε_1 (ω) with temperature can be attributed to the fact that the polarization is connected with the thermal motion of electron [38] so electrons cannot orient themselves at low temperatures. When the temperature is increased, the orientation of electrons is facilitated and this increases the value of polarization and this increases ε_1 (ω) with increasing temperature [39].

Fig. 9 shows the variation of the real part of dielectric constant with temperature at different frequencies. From this figure, the values of ε_1 (ω) increase with increasing temperature with a peak at 363 K. With increasing frequency, the intensity of this peak is decreased and becomes less pronounced. A peak in the permittivity of the sample is observed, where the permittivity reaches a constant value (the low frequency static permittivity) at sufficiently high temperature. Such a process is characterized by an asymmetrical dielectric loss peak. This type of behavior may be due to disorder in the lattice, which is the result of a shift of ion from one site to another. Although a disorder in lattice does not lead by itself to the appearance of carriers, it substantially facilitates their formation. The reason for this is the increase of ε_1 (ω) which is caused by the disorder and which weakens the coulomb interaction between the ion that departs to another unit cell and leaves behind a vacancy. As a result, transition from a state of low ε_1 (ω) to state of high ε_1 (ω) occur with increasing temperature [40]. A similar behavior is observed for the variation of ε_2 (ω) with temperature from Fig. 10. From this figure, it is observed that ε_2 (ω) increases with increasing temperature, going to peak at 363 K and then continues to the increase.

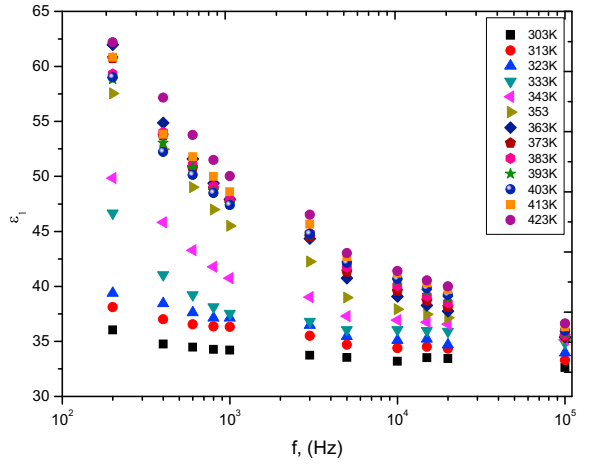

Fig. 7. The frequency dependence of ε_1 (ω) at different temperatures for C.I. Basic Violet 10 dye.

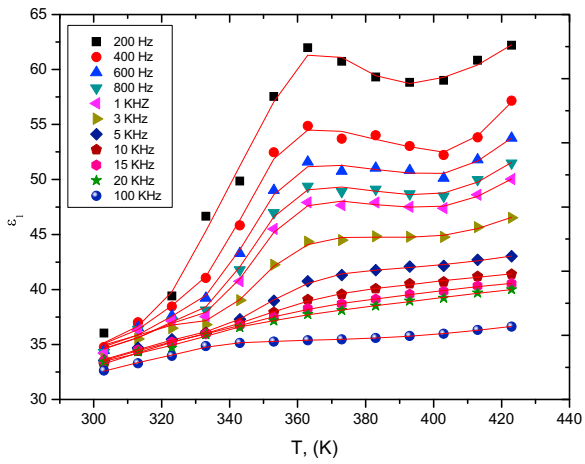

Fig. 9. Variation of ε_1 (ω) with temperature at different frequencies for C.I. Basic Violet 10 dye. The solid lines represented smoothing of the experimental data.

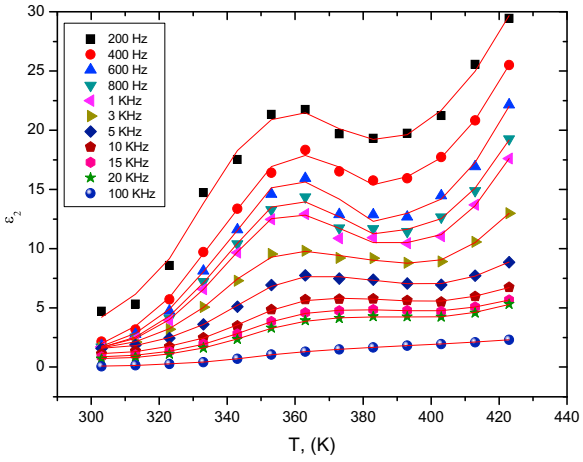

Fig. 10. Variation of $\varepsilon_2(\omega)$ with temperature at different frequencies for C.I. Basic Violet 10 dye. The solid lines represented smoothing of the experimental data.

4. Conclusions

The electrical and dielectrical properties of Basic Violet 10 dye have been investigated. The alternating current and direct current conductivity mechanisms of Basic Violet 10 dye were analyzed. The density of the localized states $N(E_F)$ was found to be $0.15 \times 10^{22} - 4.4 \times 10^{22}$ eV^{-1} cm^{-3} within the studied range of temperatures and frequencies. The dielectric relaxation mechanism for the dye was explained in terms of dependence on temperature and frequency. Hence, C.I. Basic Violet 10 is an organic semiconductor and its dielectric relaxation mechanism is temperature-dependent.

References

[1] Kubin RF, Fletcher AN. J Lumin 1982;27:455.
[2] Casey KG, Quitevis EL. J Phys Chem 1988;92:6590.
[3] Snare MJ, Treloar FE, Ghiggino KP, Thistlethwaite PJ. J Photochem 1982; 18:335.
[4] Kim HN, Lee MH, Kim HJ, Kim JS, Yoon J. Chem Soc Rev 2008;37:1465.
[5] Chun Liu, Zhiguo Zhou, Yuan Gao, Hong Yang, Baoguo Li, Fuyou Li, et al. Sci China Ser B-Chem 2009;52:760.
[6] Karatas S, Cakar M. Synth Met 2009;159:347.
[7] Boltcher CJF, Bordewijk P. Theory of electric polarization. 2nd ed., vols. I and II. New York: Elsevier; 1978.
[8] McCrum NG, Readond BE, Williams G. An elastic and dielectric effects in polymeric solids. New York: Wiley; 1967.
[9] Komilla Suri, Annapoorni S, Tandon RP. J Non-Cryst Solids 2003;332:279.
[10] Abd El Wahed MG, Metwally SM. Mater Chem Phys 2002;1:9507.
[11] Mzenda VM, Goodman SA, Auret FD, Prinsloo LC. Synth Met 2002; 129:279.
[12] Moharram MA, Salman M, El-Gendy HM. J Appl Polym Sci 1998; 168:2049.
[13] Venkatachalam S, Rao KVC, Manoharan PT. Polymer 1989;30:1633.
[14] Mzenda VM, Goodman SA, Auret FD. Synth Met 2002;127:285.
[15] Yakuphanoglu F, Gorgulu AO, Cukurovali A. Physica B 2004;353:223.
[16] Bertolassi V, Ferretti V, Gilli P, Gilli G, Issa YM, Sherif OE. J Chem Soc Perkin Trans 1993;2:2223.
[17] Bertolasi V, Nanni L, Gilli P, Ferretti V, Issa YM, Sherif OE. New J Chem 1994; 18:251.
[18] Yakuphanoglu F, Erol I. Physica B 2004;352:378.
[19] Elliott SR. Adv Phys 1987;36:135.
[20] Afifi MA, Bekheet AE, Abd El Wahabb E, Atyia HE. Vacuum 2001;61:9.
[21] Mott NF, Davis EA. Electronic processes in non-crystalline materials. Oxford: Clarendon Press; 1971.
[22] Bhattacharyya S, Saha SK, Chakravorty M, Mandal BM, Chakravorty D, Goswami K. J Polym Sci Polym Phys 2001;39:1935.
[23] Ghosh A. Phys Rev B 1990;41:1479.
[24] Ghosh A. Phys Rev B 1990;42:5665.
[25] Long AR. Adv Phys 1982;31:553.
[26] Pike GE. Phys Rev B 1972;6:1572.
[27] Elliott SR. Philos Mag B 1978;37:135.
[28] Elliott SR. Philos Mag B 1978;36:129.
[29] Chaudhuri BK, Chaudhuri K, Som KK. J Phys Chem Solids 1989;50:1147.
[30] Austin IG, Mott NF. Adv Phys 1969;18:41.
[31] Reda SA. Dyes Pigm 2007;75:526.
[32] Yakuphanoglu F, Evin E, Okutan M. Physica B 2006;382:285.
[33] Moynihan CT, Boesch LB, Laberge NL. Phys Chem Glasses 1973;14:122.
[34] Macedo PB, Moynihan CT, Bose R. Phys Chem Glasses 1972;13:171.
[35] Kurien S, Mathew J, Sebastian S, Potty SN, George KC. Mater Chem Phys 2006; 98:470.
[36] Bunget I, Popescu M. Phys solid dielectric. New York: Elsevier; 1984.
[37] Anantha PS, Harihanan K. Mater Sci Eng B 2005;121:12.
[38] Deger D, Ulutas K. Balkan Phys Lett 2000;8:48.
[39] Seyam MAM. Appl Surf Sci 2001;181:128.
[40] Yakuphanoglu F, Aydogdu Y, Schatzschneider U, Rentschler E. Solid State Commun 2003;128:63.